Discrimination different lithological units using a remote sensing application: A case study in the Dokan Area, Kurdistan Region – Iraq

Azhar Kh. S. Bety ✉ iD

University of Sulaimani, College of Science, Department of Geology, Tasluja Str. 1,
Zone 501 Sulaimania, As Sulaymaniyah, Kurdistan Region, Iraq

Abstract: This study discriminates different lithological units of the Dokan Area, Kurdistan Region, NE-Iraq, using rapid-eye satellite data by image enhancement techniques, namely the false colour composite (FCC), optimum index factor (OIF), minimum noise fraction (MNF), principal component analysis (PCA) and band ratio (BR). Results of analyses show that the FCC (R: 5; G: 4: B: 1); MNF (R: 2, G: 3, B: 5); PCA (R: 5, G: 2, B: 1), and band ratio (R: 5/4, G: 2/1, B: 5/3) are the best to different geological formations. The results are confirmed in the field support with the geological maps available for the area. Geological formations appeared as a result of the collision process between the Arabian plate and the Iranian plate. In general, the study area is mountainous, which is usually represented by anticline folds with the main NW – SE trend in the study area, with very a rugged relief mainly due to the continuous collision between the Arabian plate and Iranian plate. The digital image processing of satellite data has demonstrated the sensor's capability and efficiency of the image processing methods in identifying and mapping geological units in the study area.

Keywords: Dokan Area, image enhancement, image transformation, lithological units, rapid eye, remote sensing

INTRODUCTION

Geological mapping is important for any geological work and provides vital information about the geology of the area. Such information can be used for several proposes. Mineral exploration and geological unites identification were considered arduous, costly, and time-consuming and relied heavily on fieldwork [RAMAKRISHNAN, BHARTI 2015]. Recently, the geographic information system (GIS) and remote sensing technologies play an important role in updating geological maps and enable to produce geological maps from satellite images.

Remote sensing provides a continuous source for geological mapping, concerning some issues that must be taken into account when mapping the distribution of rock structures, such as the absence of clouds, vegetation, and atmospheric effects that can affect the sensor reading of surface reflectivity. Recently, satellite images have the potential to survey natural resources including vegetation coverage, rock types, and minerals [RAJENDRAN *et al.*

2014; RAJENDRAN, NASIR 2015]. In geology, identification of important structures, mapping of rock units and natural resources are important applications of remote sensing [OTHMAN, GLOAGUEN 2014]. Recently, many researchers have expressed interest in the subject of mapping rock units or identifying mineral deposits through different image processing techniques [HAMIMI *et al.* 2020; KUMARI *et al.* 2014; OTHMAN, GLOAGUEN 2014]. However, there are very few studies dealing with the application of the techniques in the geological mapping of northern Iraq [OTHMAN, GLOAGUEN 2014; 2017]. The Dokan Area has been investigated at a scale of 1:100,000 by SISSAKIAN [2013], who divided the Dokan Area into several units. However, the deficiencies of the previous geological map result from restricted accessibility of the area as a result of its relief as well as the spread of mined areas (remains from the Iran-Iraq war) over the study area. Therefore, the unreachable areas have not been well described.

The objective of the present paper is to discriminate between rock units (formations) using rapid-eye satellite images

which have 5 m spatial resolution. This study attempts to map geological formations of the Dokan Area, Kurdistan Region, NE-Iraq. The results of the research were confirmed through field work and available geological maps.

MATERIALS AND METHODS

STUDY AREA

The Dokan Area is located in the Kurdistan Region, northeast-Iraq, about 80 km Northwest of the Sulaymaniyah City. It lies between longitudes 44°50' E and 45°00' E and latitudes 35°55' N and 36°00' N (Fig. 1). It is part of the Zagros Fold – Thrust Belt of the Outer Platform of the Arabian Plate [AMEEN, GAHRIB 2010; FOUAD, 2015; KOYI et al. 2000]. It includes many mountains that reflect the influence of the region by the Alpine orogeny, which was formed by the collision between the Eurasian and the Arabian plates, and the closure of the Neo-Tethys [ALAVAI 1994; SISSAKIAN 2013]. The anticlines within the selected area are mostly long and narrow with the NW–SE trend. The selected high mountains area occupies ~96 km^2. Its elevation ranges between 360 m and 1174 m a.s.l.

Tectonically, the fundamental framework of the stratigraphy and structure of the study area is influenced by the positioning of Iraq within the tectonic units of north Iraq. The Dokan Area is located within the High Folded Zone (HFZ) of the unstable Arabian Plate platform [FOUAD 2015]. The HFZ includes several structural features such as folds, faulting (mainly thrust with some normal faults). The majority of these structural features have the NW–SE positioning. The area represents part of the Khalikan anticline. It is mostly made up of high amplitude anticlines, many of which are asymmetrical, with the southwestern limb being steeper than the north-eastern one [SISSAKIAN et al. 2016].

Stratigraphy, the formations (Fn) are ranging from Cretaceous to Cenozoic in age and overlain by different types of Quaternary sediments. It includes the following, well exposed rock of Cretaceous units, which are Qamchuqa, Kometan,

Shiranish, and Tanjero, and Tertiary unites, which are Kolosh, Khurmala (which is equivalent to Sinjar formation), Gercus and Pila Spi formation (Fig. 2, Tab. 1).

SATELLITE IMAGE AND SOFTWARE

In this work, the 2015 rapid-eye data were used to distinguish the rock units of the study area. Five bands of rapid eye with the spatial resolution of 5 m were used (Tab. 2).

ENVI, ELWIS, and ArcGIS are the main software apps used in this study. Beside the atmospheric and radiometric corrections, the ENVI 5.3 software was used to pre-process the data, such as layer stack and subset. It was also used to conduct the FCC, MNF, PCA and BR. ELWIS was used to find the OIF and Arc GIS to prepare the base and final maps produced from digital processing.

IMAGE PROCESSING

Digital processing is an important aspect of geological studies, especially those that rely on satellite imagery. Image processing is one of the methods that aim to improve satellite images through various processes, which may be MNF, PCA and BR methods used at the present time for the purpose of obtaining better contrast to distinguish the image contents and extract useful information. The digital data processing used in this study included several operations, which were represented as follows.

• **False colour composite (FCC) images**

Each band of a multispectral image might well be displayed as a grey scale image or as a combination of three RGB bands as a colour composite image. The composite 3, 2, 1 as RGB true colour, while the false colour composite FCC is an exemplification of three or more, the multispectral image produced using selected bands from ranges of red, green and blue, infrared. Different FCCs that can be used to highlight different rock units with other features on the image. The processing was also relied upon to improve the images resulting from other digital processing like MNF, PCA, and BR.
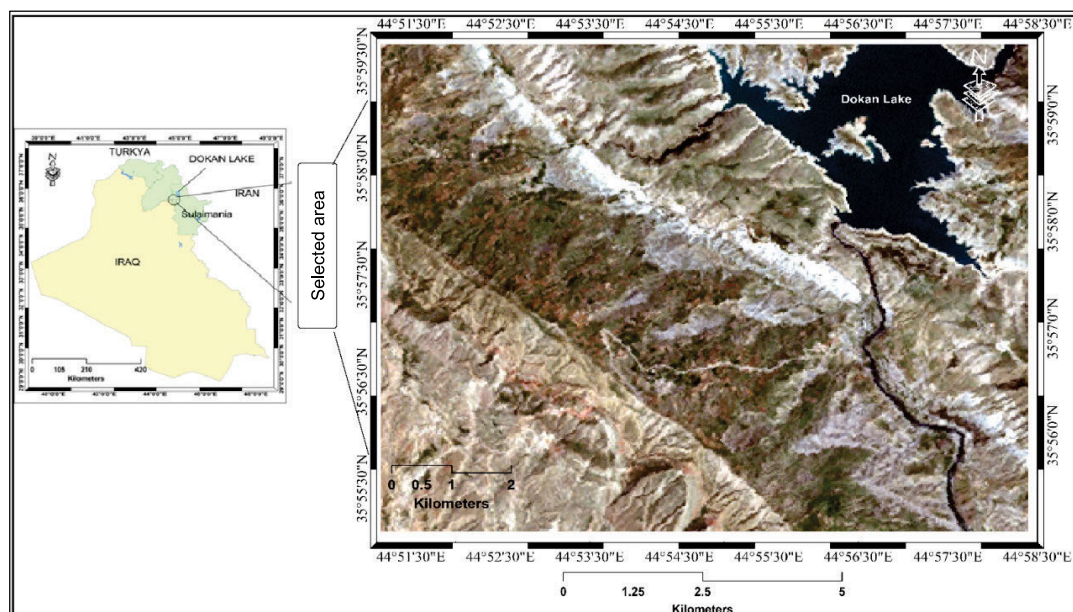

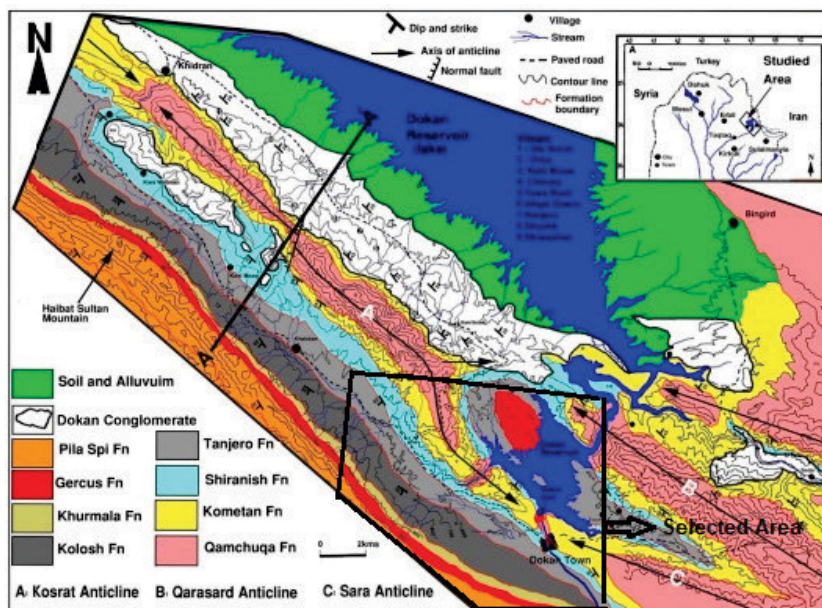**Fig. 1.** The location of the study area – satellite image (R: 3, G: 2, B: 1); source: own elaboration based on Google Earth

Fig. 2. Geological map of the study area; Fn = formation; source: KARIM and TAHA [2012], modified

Table 1. The rock description of the formations within study area

Formation	Rock description
Qamchuqa	hard and massive dolomite, which is highly jointed and fractured
Kometan	hard, well-bedded, highly jointed and fractured stylolitic limestone
Shiranish	soft marl and argillaceous limestone
Tanjero	sandstone and marl beds
Kolosh	shales, claystones, sandstones and marly limestone
Khurmala	massive and fine crystalline limestone
Gercus	typical rocks include claystone, sandstone, and siltstone
Pila Spi	well-bedded dolomite and dolomitic limestone

Source: own elaboration.

Table 2. Rapid-eye's wavelength of used bands

Band number and name	Band wavelength (nm)
1 – blue	440–510
2 – green	520–590
3 – red	630–680
4 – red edge	690–730
5 – NIR	760–850

Explanation: NIR = near infrared.
Source: own elaboration.

- **Minimum noise fraction (MNF) images**

The MNF is a processing consisting of two methods which are extracted by rotations of principal components and noise removal processing [GREEN et al. 1988]. MNF transforms are rotated to reveal the inherent dimensionality of image data, to isolate noise in the data, as well as to reduce the computational demands of subsequent digital processing [BOARDMAN, KRUSE 1994]. Noise removal has been studied in many types of research and several methods have been proposed [QIAN et al. 2008]. The MNF is applied to surface reflectance data to assess the spatial variability of different rock units.

- **Principal component analysis (PCA) images**

The PCA is similar to the MNF transformation. Previously, there were a number of algorithms and methods applied to remove noise [SYARIF, KUMARA 2018]. The principal component analysis was used to reduce the amount of redundant information in bands highly correlated to image bands [GASMI et al. 2016]. The PCA provides more details than other traditional methods because the output data are uncorrelated [JENSEN 2005].

- **Band ratio (BR) images**

The BR method enhances the contrast between targets or features based on dividing the reflectance for the one band pixels by the same pixels in other bands [AMER et al. 2010; RAJENDRAN, NASIR 2014]. The BR has been used by researchers in many fields, most of them related to rock units and hydrothermal alteration identification [AMER et al. 2010]. Rocks have different reflectivity due to different mineral components, as well as different wavelengths, as they can have high reflectivity in a certain part of the wavelength and low reflectivity in another part. The band with high reflectivity is divided into the band with low reflectivity to achieve the best result. This process proved a great potential in separating geological formations.

- **Optimum index factor (OIF)**

The OIF is a statistic number that can be used to determine the best combination of three bands in a satellite image for creating an RGB colour composite. The OIF is calculated using the total variance and correlation within and between all of the dataset's band combinations. The OIF method was created for Landsat TM data, but the definition and methodology can be used for any multilayer dataset [KIENAST-BROWN, BOETTINGER 2010]. This method was adopted to choose the best RGB combination from the bands resulting from digital processors that were

applied, but this method did not give the best results compared with the visual interpretation. Therefore, the resulting RGB image composition was based on visual interpretation to determine the best combination of RGB to isolate the rock units within the study area

FIELD VALIDATION

The results were validated using a geological map and a field survey. Moreover, GPS ground points were used to match the formations of contacts between the field work and interpreted images. The field work showed a limited area of the Qamchuqa formation and the Khurmala formation within the study area, while the boundaries of these formations were not determined on the geological map [Sissakian, Fouad 2014].

RESULTS AND DISCUSSION

FORMATION DETERMINED BY THE FCC

In this study, the false colour composite (R: 5, G: 4, B: 1) using the spectral bands of rapid eye were developed (Fig. 3). The FCC clearly shows the contacts between Shiranish and Tangier formations, the Shiranish formation appears with high reflectivity white colour, while the Tanjero formation appears with medium reflectivity and dull colour. Also, Khurmala formation is clear, its contact with Kolosh formation is so clear. FCC (R: 5, G: , B: 1) shows Qamchuqa Formation with dark green colour. The near-infrared and short-wave infrared bands showed good potential in isolating some rock units through the FCC method.
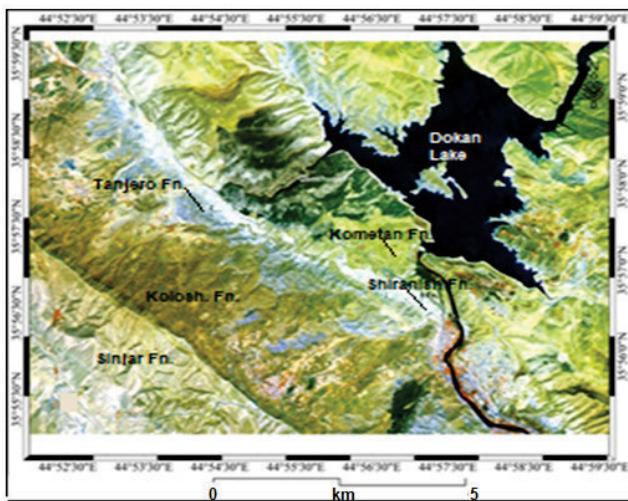

Fig. 3. Image of false colour composite with RGB 5 4 1; source: own study

MAPPING OF GEOLOGICAL FORMATIONS BY IMAGE TRANSFORMATION METHOD

This method is not widely used to discriminate different geological formations compared to the BR method, but good results in this study encourage its adoption in isolating rock units in areas similar to the study area from a topographical and geological point of view.

Minimum noise fraction (MNF)

The results of the MNF showed geological formations in different colours. The MNF (R: 2, G: 3, B: 5) image was selected as the best image to show the distribution of the formations in the selected area depending on the MNF composites (Fig. 4). Most of the formations in the study area are clearly shown with the MNF in the FCC (R: 2, G: 3, B: 5).
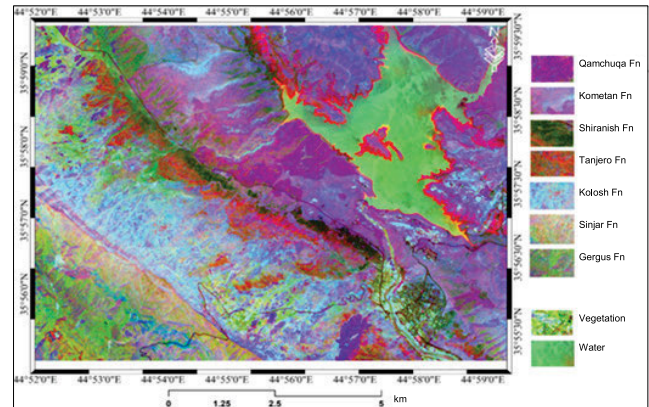

Fig. 4. Imagery of the minimum noise fraction (R: 2, G: 3, B: 5); source: own study

Principal component analysis (PCA)

Five components were extracted from the rapid-eye image. The first PC contains the largest percentage of information and the second PC contains the second-largest information set, and so on; the last PC appears noisy because they contain most of the little variance. Much of these components are due to noise in the original spectral data. Since PC1 and PC2 gave more information and details about the geological formations than the other, it was possible to distinguish several rock formations (Fig. 5). Many false colour images were formed from PCA and it was found that the best band combination is: (R: 5, G: 2, B: 1), where most of the geological formations appeared very clearly (Fig. 6).

FORMATION DETERMINED BY BAND RATIO (BR)

To examine which combinations are the most suitable and relevant for the geological settings of the selected area, 20 bands ratios were formed depending on the input bands of the rapid-eye satellites. After examining different combinations of band ratios, the FCC of band ratio (R: 5/4, G: 2/1, B:5/3) was selected as the best images for the discrimination of the formations (Fig. 7).

ACCURACY OF THE RESULTS

The field GPS points of the contacts between different geological units were projected on the produced images to ensure the accuracy of the results. The results showed a high possibility of digital manipulation in drawing and separating boundaries between different formations. The contacts between the formation and some photos are shown within the 3D image (Fig. 8).
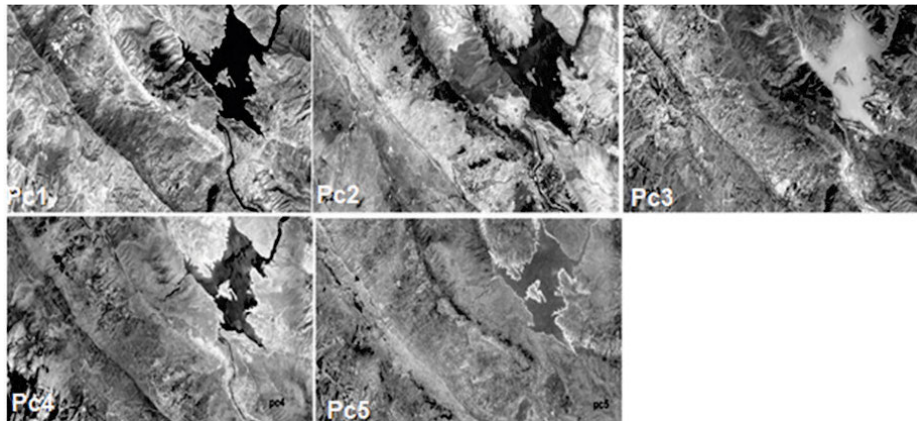
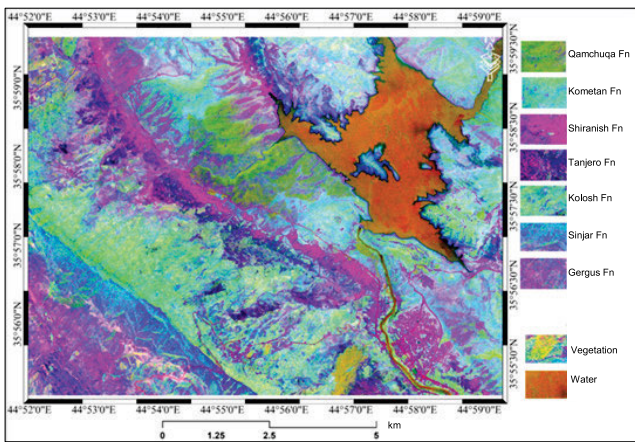**Fig. 5.** Five principal component bands of the rapid-eye image of the study area; source: own study

Fig. 6. The colour composites of the principal component analysis (R: 5, G: 2, B: 1) image; source: own study
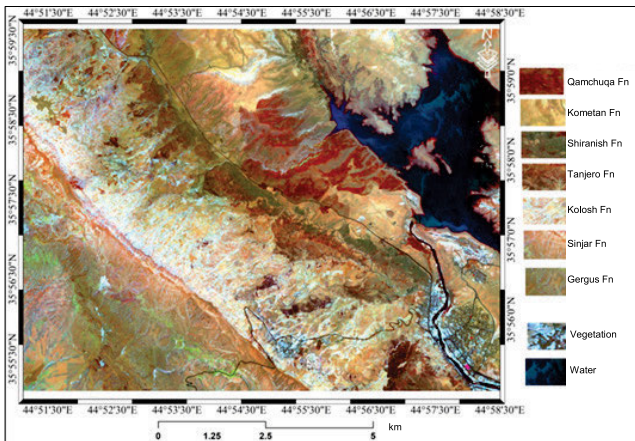

Fig. 7. False colour composite of ratio (R: 5/4, G: 2/1, B: 5/3) image within the study area; source: own study

CONCLUSIONS

Image processing helps a lot in highlighting boundaries of many geological units which are difficult to distinguish with individual bands. The applied digital processing gave good and convergent results for the process of separating the geological units within part of the Dokan Area. In general, the optimum index factor (OIF) and the best combination of RGB did not produce good results for separating the geological formations from each other,
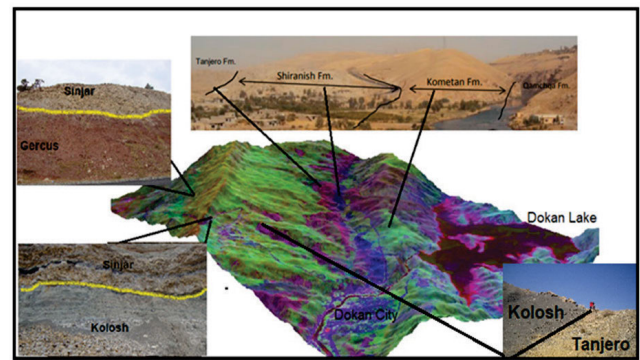

Fig. 8. 3D image with some field photos; source: own study

so the selection of the best combination involved many attempts to reach satisfactory results. The boundaries separating the Tanjero and Kolosh formations within the study area are covered in most parts by recent sediments, so it was difficult to determine the boundary between them in some parts of the study area.

The study demonstrated the importance of adopting satellite image digital data in updating geological maps, especially those that cover large areas. As the Qamchuqa and Khurmala formations were not indicated in the geological map due to the topographical nature of the area or too limited spread of these formations within the study area, it was difficult to draw the boundaries of these formations on such maps. At the same time, these two configurations can be distinguished on the visual data after performing digital processing. In general, the results of digital processing are close to the satellite images approved in the study.

REFERENCES

Alavai M. 1994. Tectonic of the Zagros orogenic belt of Iran: New data and interpretations. Tectonophysics. Vol. 229(3) p. 211–238. DOI 10.1016/0040-1951(94)90030-2.

Ameen F.A., Gahrib H. 2010. Cretaceous sequence stratigraphy of Westrenzagros Outcrops from Kurdistan Region, N. Iraq. Conference Proceedings GEO 2010, cp-248. DOI 10.3997/2214-4609-pdb.248.343.

Amer R., Kusky T., Ghulam A. 2010. Lithological mapping in the Central Eastern Desert of Egypt using ASTER data. Journal of

African Earth Sciences. Vol. 56(2–3) p. 75–82. DOI 10.4236/ojg. 2017.78080.

Boardman J.W., Kruse F.A. 1994. Automated spectral analysis: A geological example using AVIRIS data, north Grapevine Mountains, Nevada. In: Proceedings, ERIM 10th Thematic Conference on Geologic Remote Sensing. Ann Arbor, MI. Environmental Research Institute of Michigan. Vol. 1 p. I-407–I-418.

Fouad S.F.A. 2015. Tectonic map of Iraq, scale 1: 1000 000. 3rd ed. 2012 [online]. Iraqi Bulletin of Geology and Mining. Vol. 11. No. 1 p. 1–7. [Access 10.09.2021]. Available at: https://www.iasj.net/iasj/download/3c7670270c9c61c1?fbclid=IwAR1LjkBZVu-BYwTwhKVn6wisu44PUOllJYbau8dShm_kFDepiRQ81LD5WQV8

Gasmi A., Gomez C., Zouari H., Masse A., Ducrot D. 2016. PCA and SVM as geo-computational methods for geological mapping in the southern of Tunisia, using ASTER remote sensing data set. Arabian Journal of Geosciences. Vol. 9(20), 753. DOI 10.1007/s12517-016-2791-1.

Green A.A., Berman M., Switzer P., Craig M.D. 1988. A transformation for ordering multispectral data in terms of image quality with implications for noise removal. IEEE Transactions on Geoscience and Remote Sensing. Vol. 26(1) p. 65–74. DOI 10.1109/36.3001.

Hamimi Z., Hagag W., Kamh S., El-Araby A. 2020. Application of remote-sensing techniques in geological and structural mapping of Atalla Shear Zone and Environs, Central Eastern Desert, Egypt. Arabian Journal of Geosciences. Vol. 13(11), 414. DOI 10.1007/s12517-020-05324-8.

Jensen J.R. 2005. Image enhancement. In: Introductory digital image processing: A remote sensing perspective. Chapt. 8. Hoboken. Prentice Hall p. 301–322.

Karim K.H., Taha Z.A. 2012. Origin of conglomeratic limestone "Dokan conglomerate" in Dokan area, Kurdistan region, NE Iraq. Iraqi Bulletin of Geology and Mining. Vol. 8(3) p. 15–24.

Kienast-Brown S., Boettinger J.L. 2010. Applying the optimum index factor to multiple data types in soil survey. In: Digital soil mapping [online]. Chapt. 30. Springer p. 385–398. [Access 10.09.2021]. Available at: https://link.springer.com/content/pdf/10.1007/978-90-481-8863-5_30.pdf

Koyi H.A., Hessami K., Teixell A. 2000. Epicenter distribution and magnitude of earthquakes in fold-thrust belts: Insights from sandbox models. Geophysical Research Letters. Vol. 27(2) p. 273–276.

Kumari S.K., Debashish C., Pulakesh D., Jatisankar B. 2014. Hyperion image analysis for iron ore mapping in Gua Iron Ore Region, Jharkhand, India. International Research Journal of Earth Sciences. Vol. 2(9) p. 1–6.

Othman A.A., Gloaguen R. 2014. Improving lithological mapping by SVM classification of spectral and morphological features: The discovery of a new chromite body in the Mawat ophiolite complex (Kurdistan, NE Iraq). Remote Sensing. Vol. 6(8) p. 6867–6896.

Othman A.A., Gloaguen R. 2017. Integration of spectral, spatial and morphometric data into lithological mapping: A comparison of different machine learning algorithms in the Kurdistan Region, NE Iraq. Journal of Asian Earth Sciences. Vol. 146 p. 90–102. DOI 10.1016/j.jseaes.2017.05.005.

Qian Y., Qiu F., Chang J., Zhang K. 2008. Visualization-informed noise elimination and its application in processing high-spatial-resolution remote sensing imagery. Computers & Geosciences. Vol. 34(1) p. 35–52. DOI 10.1016/j.cageo.2007.02.006.

Rajendran S., Nasir S. 2014. Hydrothermal altered serpentinized zone and a study of Ni-magnesioferrite–magnetite–awaruite occurrences in Wadi Hibi, Northern Oman Mountain: Discrimination through ASTER mapping. Ore Geology Reviews. Vol. 62 p. 211–226. DOI 10.1016/j.oregeorev.2014.03.016.

Rajendran S., Nasir S. 2015. Mapping of high pressure metamorphics in the As Sifah region, NE Oman using ASTER data. Advances in Space Research. Vol. 55(4) p. 1134–1157. DOI 10.1016/j.asr.2014.11.026.

Ramakrishnan D., Bharti R. 2015. Hyperspectral remote sensing and geological applications. Current Science. Vol. 108. No. 5 p. 879–891. DOI 10.18520/CS/V108/I5/879-891.

Sissakian V., Ahad A.A., Al-Ansari N., Hassan R., Knutsson S. 2016. The regional geology of Dokan area, NE Iraq. Journal of Earth Sciences and Geotechnical Engineering. Vol. 6(3) p. 35–63.

Sissakian V.K. 2013. Geological evolution of the Iraqi Mesopotamia Foredeep, inner platform and near surroundings of the Arabian Plate. Journal of Asian Earth Sciences. Vol. 72 p. 152–163. DOI 10.1016/j.jseaes.2012.09.032.

Sissakian V.K., Fouad S.F. 2014. Geological map of Sulaimaniyah Quadrangle, scale 1: 250000. Baghdad, Iraq. Iraq Geological Survey Publications. DOI 10.17656/jzs.10477.

Syarif A.M., Kumara I.S.W. 2018. The effect of minimum noise fraction on multispectral imagery data for vegetation canopy density modelling. Geoplanning: Journal of Geomatics and Planning. Vol. 5(2) p. 251–258. DOI 10.14710/geoplanning.5.2.251-258.